chemistry

MDPI

Article

Selective Styrene Oxidation Catalyzed by Phosphate Modified Mesoporous Titanium Silicate

Rupak Chatterjee [1,†], Avik Chowdhury [1,†], Sudip Bhattacharjee [1], Rajaram Bal [2] and Asim Bhaumik [1,*]

[1] School of Materials Sciences, Indian Association for the Cultivation of Science, 2A & 2B Raja S. C. Mullick Road, Jadavpur, Kolkata 700032, India
[2] Light Stock Processing Division, CSIR—Indian Institute of Petroleum, Dehradun 248005, India
* Correspondence: msab@iacs.res.in
† These authors contributed equally to this work.

Abstract: Selective oxidation of organics over an efficient heterogeneous catalyst under mild liquid phase conditions is a very demanding chemical reaction. Herein, we first report the modification of the surface of mesoporous silica MCM-41 material by phosphate for the efficient incorporation of Ti(IV) in the silica framework to obtain highly ordered 2D hexagonal mesoporous material STP-1. STP-1 has been synthesized by using tetraethyl orthosilicate, triethyl phosphate, and titanium isopropoxide as Si, P, and Ti precursors, respectively, in the presence of cationic surfactant cetyltrimethylammonium bromide (CTAB) under hydrothermal conditions. The observed specific surface area and pore volume of STP-1 were 878 m^2g^{-1} and 0.75 ccg^{-1}, respectively. Mesoporous STP-1 has been thoroughly characterized by XRD, FT-IR, Raman spectroscopy, SEM, and TEM analyses. Titanium incorporation (Ti/Si = 0.006) was confirmed from the EDX analysis. This mesoporous STP-1 was used as a heterogeneous catalyst for the selective oxidation of styrene into benzaldehye in the presence of dilute aqueous H_2O_2 as an oxidizing agent. Various reaction parameters such as the reaction time, the reaction temperature, and the styrene/H_2O_2 molar ratio were systematically studied in this article. Under optimized reaction conditions, the selectivity of benzaldehyde could reach up to 93.8% from styrene over STP-1. Further, the importance of both titanium and phosphate in the synthesis of STP-1 for selective styrene oxidation was examined by comparing the catalytic result with only a phosphate-modified mesoporous silica material, and it suggests that both titanium and phosphate synergistically play an important role in the high selectivity of benzaldehyde in the liquid phase oxidation of styrene.

Keywords: titanium silicate; MCM-41; styrene oxidation; benzaldehyde; phosphate modification

Citation: Chatterjee, R.; Chowdhury, A.; Bhattacharjee, S.; Bal, R.; Bhaumik, A. Selective Styrene Oxidation Catalyzed by Phosphate Modified Mesoporous Titanium Silicate. *Chemistry* **2023**, *5*, 589–601. https://doi.org/10.3390/chemistry5010042

Academic Editors: José Antonio Odriozola and Hermenegildo García

Received: 10 February 2023
Revised: 7 March 2023
Accepted: 8 March 2023
Published: 10 March 2023

1. Introduction

Oxidation of olefin is considered to be one of the primitive reactions in synthetic organic chemistry [1]. A series of value-added chemicals such as epoxides, diols, and carbonyl compounds are obtained as a result of olefin oxidation under mild reaction conditions [2,3], and often, they are found as key precursors for the targeted organic synthesis in different chemical industries. Thus, selective catalytic oxidation under eco-friendly conditions has gained significant industrial importance over the years [4–6]. The traditional synthetic route for this oxidation reaction surprisingly still involves hazardous pathways such as ozonolysis [7], which can lead towards tremendous threat to the Earth and atmospheric safety [8]. Thus, the global scientific community is exploring alternative safe routes over the years to invent suitable heterogeneous catalysts in the selective oxidation reactions. Scientists have paid particular attention to developing sustainable and economical as well as eco-friendly strategies on oxidation of olefins. In this context, epoxidation of olefins through a catalytic-peroxide-mediated pathway [9–11] is currently regarded as one of the important alternative routes. Strategies such as peroxo-mediated olefin conversion

have gained significant attention in this regard. The use of hydrogen peroxide in this context is very significant due to its benefits such as operating ease, cost effectiveness, high synthetic yields, and remarkable safety [12], as this reaction involves generation of water as the only byproduct. Although initially the process starts with mainly generation of homogeneous catalysts, the high cost and no scope of recyclability associated with this process [13] motivate scientists to shift the process towards a heterogeneous [14] pathway. The main scientific interests growing on development of an olefin oxidation strategy through a heterogeneous approach have come up with some excellent catalysts with good reproducibility. Thus, today, transition-metal-catalyzed oxidation [15,16] is the most successful reaction for the synthesis of epoxides. In this context, Stack group has developed a cationic manganese complex to effectively epoxidize electron-deficient olefins [9], and Sun group reported another manganese-based catalyst [17] capable of generating epoxide. Various other transition-metal-based catalysts [18–21] are also under rapid progress in this field. Although very diverse research already has been carried out till now, the process still lags some serious drawbacks due to the limitations such as cost effectiveness, tough synthetic procedures, lack of recyclability, and low catalytic stability, demanding more catalyst modification for the accomplishment of this oxidation reaction.

Porous nanomaterials [22] are currently attracting considerable attention to the scientific world due to their widespread applicability in a variety of real-world issues. The excellent fundamental material properties such as the high specific surface area, ease of synthetic methodologies, enhanced chemical stability, and tunability of the chemical compositions are responsible for their wide range of potential applicability in solving energy and environmental problems such as gas sorption [23], sensing [24], waste water remedies [25], and removal of toxic pollutants from natural resources [26]. In this scenario, ordered mesoporous silica materials are considered to be one of the promising candidates in the family of porous materials. Starting from the discovery by the Mobil researchers in 1992 [27], a vast amount of research has been carried out so far, which come up with some excellent members of this class such as SBA-15 [28], SBA-16 [29], and single-crystalline MCM-48 [30].

Although a large number of heteroelements can be incorporated into the mesoporous silica framework, incorporation of tetrahedral Ti(IV) in the silicate framework offers unique advantages in designing a reactive heterogeneous catalyst to carry out a large spectrum of oxidation reactions under mild reaction conditions. Extensive research has already been carried out by using an MFI-type microporous titanium silicate catalyst for this purpose. For example, Lamberti et al. have reported TS-1 as a single-site catalyst in this context [31], Coperet and coworkers have reported efficient epoxidation over dinuclear sites in titanium silicalite-1 [32], and Shen group have reported zeolite-modified TS-1 in 1-hexene epoxidation reaction [33]. High stability of titanium-hydroperoxo species, which are generated in the liquid phase oxidation reactions in the presence of H_2O_2, plays a crucial role in these oxidation reactions. Further, considering enhanced affinity of titanium towards phosphates [34], we have explored the possibility of phosphate modification in the synthesis of a mesoporous titanium silicate framework to enhance its catalytic activity. We have fabricated a 2D hexagonal phosphate-modified mesoporous titanium silicate material STP-1 containing reactive Ti(IV) species which was incorporated into the silica framework. STP-1 showed excellent catalytic activity in the selective oxidation of styrene into benzaldehyde under very mild reaction conditions using H_2O_2 as an oxidant. This high selectivity of STP-1 for benzaldehyde could be attributed to the synergistic effect of titanium and phosphate species. We have also synthesized the phosphate containing mesoporous silica material (SP-1) and used the same in this catalytic reaction.

2. Materials and Methods

2.1. Chemicals

Cetyltrimethylammonium bromide (CTAB), tetraethyl orthosilicate (TEOS), triethyl phosphate, and titanium isopropoxide were purchased from Sigma Aldrich, Bangalore,

India. Dilute aqueous H_2O_2 (25%) was purchased from Merck, Bangalore, India. All others reagents and solvents were used without any further purification.

2.2. Instrumentation

The mesophase formation and crystalline/amorphous nature of the particle of the as-synthesized and calcined materials were investigated by small angles (2θ, 1°–5°) and wide angles (2θ, 10°–80°) powder X-ray diffraction analysis, respectively, using a Bruker D8 advance X-ray diffractometer (Germany). The bonding connectivity and the state of titanium incorporation in the materials were scrutinized by Fourier-transform infrared spectroscopy (FTIR) using a Shimadzu FT-IR 8400S (Kyoto, Japan) instrument where the samples were prepared in KBr pellets. UV-visible spectroscopic analysis was performed for studying the titanium incorporation and spectral properties. All the UV-visible spectra were taken in Shimadzu 2401PC (Kyoto, Japan). Raman spectroscopy was measured by a Horiba T64000 instrument. JEOL JEM 2100F was used for the investigation of microscopic dimension of the particle in STP-1, and the crystal fringe pattern of the particle was investigated by ultra-high-resolution TEM. The particle assembly and elemental analysis in STP-1 analyzed by field-emission scanning electron microscopy (FE-SEM) using a JEOL JSM-7500 F (Tokyo, Japan) scanning electron microscope. The presence of permanent porosity in STP-1 was analyzed by N_2 sorption analysis at 77 K using a Anton Paar QuantaTec (Boynton Beach, FL, USA) iSorb HP1 instrument. The formation of the catalytic products and the yield of the products were analyzed using gas chromatography analysis (GC) with the help of Centurion Scientific (New Delhi, India) GC, where an FID was used as a detector.

2.3. Synthesis of STP-1

STP-1 was synthesized through a hydrothermal synthesis route in an autoclave using an autogenous pressure at 85 °C. In a typical synthetic route, 0.54 g CTAB, 10.6 g H_2O, and 5.7 g aqueous ammonia (pH = 11.8) were taken in the teflon chamber of the autoclave followed by vigorous stirring for 2 h. Then, 1.038 g TEOS (4.984 mmol) was added followed by a subsequent addition of 177 mg of titanium isopropoxide (0.623 mmol), and finally, 113 mg of triethyl phosphate (0.623 mmol) was added as a phosphate source. The final reaction mixture was allowed to stir for another 4 h; finally, the mixture was kept in 85 °C in a static condition for 48 h. After the completion of the reaction, the white precipitate was filtered and thoroughly washed with water. After drying at a 70 °C oven, it was kept for calcination at 550 °C for 6 h. A finely powdered white color material was obtained.

The phosphate-modified mesoporous silica without titanium (SP-1) was synthesized by the same procedure of STP-1. Here, 0.54 g CTAB, 10.6 g H_2O, and 5.7 g aqueous ammonia (pH = 11.8) were taken in the teflon chamber of the autoclave followed by vigorous stirring for 2 h. Then, 1.038 g TEOS (4.984 mmol) was added followed by a subsequent addition of 113 mg of triethyl phosphate (0.623 mmol) added as a phosphate source. The final reaction mixture was allowed to stir for another 4 h; finally, the mixture was kept in 85 °C in a static condition for 48 h. After the completion of the reaction, the white precipitate was filtered and thoroughly washed with water. After drying at a 70 °C oven, it was kept for calcination at 550 °C for 6 h. A finely powdered white color material was obtained.

2.4. Styrene Oxidation Catalysis

Styrene (0.572 mL, 5 mmol), hydrogen peroxide (0.142 mL, 5 mmol), a catalyst (52 mg, 10 wt%), and acetonitrile (5 mL) as a solvent were added in a two-necked round bottom flask. The whole reaction mixture was heated at different temperatures for several time intervals. The reaction was monitored by collecting the aliquot of the reaction mixture at different time intervals, and the catalyst was separated by centrifugation. The composition of the product into the reaction mixture was analyzed by gas chromatography.

2.5. Catalyst Activation

Prior to the all catalytic reactions, the catalyst needed to be activated for the removal of trapped solvent molecules, which affected the catalytic activity due to the blocking of active sites. Hence, the material was activated by heating at 130 °C for 2 h for each catalytic cycle. To measure the catalytic recyclability, the catalyst was again isolated, dried and activated by the same procedure.

3. Results

Phosphate-modified mesoporous titanium silicate material STP-1 was synthesized by using CTAB as a structure directing agent (SDA) under hydrothermal conditions in the presence of aqueous ammonia. The small-angle powder X-ray diffraction (PXRD) pattern of STP-1 material is shown in Figure 1a, which was well matched with the pure silica MCM-41 material [35]. In the PXRD pattern, there were four diffractions in the 2θ range of 0.5°–10° corresponding to the reflection of the planes 100, 110, 200, and 210, respectively [36,37]. The diffraction peaks remained same after the calcination of the material at 550 °C that concluded that the hexagonal arrays of the 2D hexagonal mesoporous structure remained intact after calcination (Figure 1a). Furthermore, the wide-angle PXRD of STP-1 material after calcination showed a broad peak around 23°, suggesting the amorphous pore wall of silica (Figure 1b). Further, it is important to mention that there was no peak corresponding to the TiO_2 phase in the STP-1 sample, which suggests that the titania species was nicely dispersed into the silica framework [38].

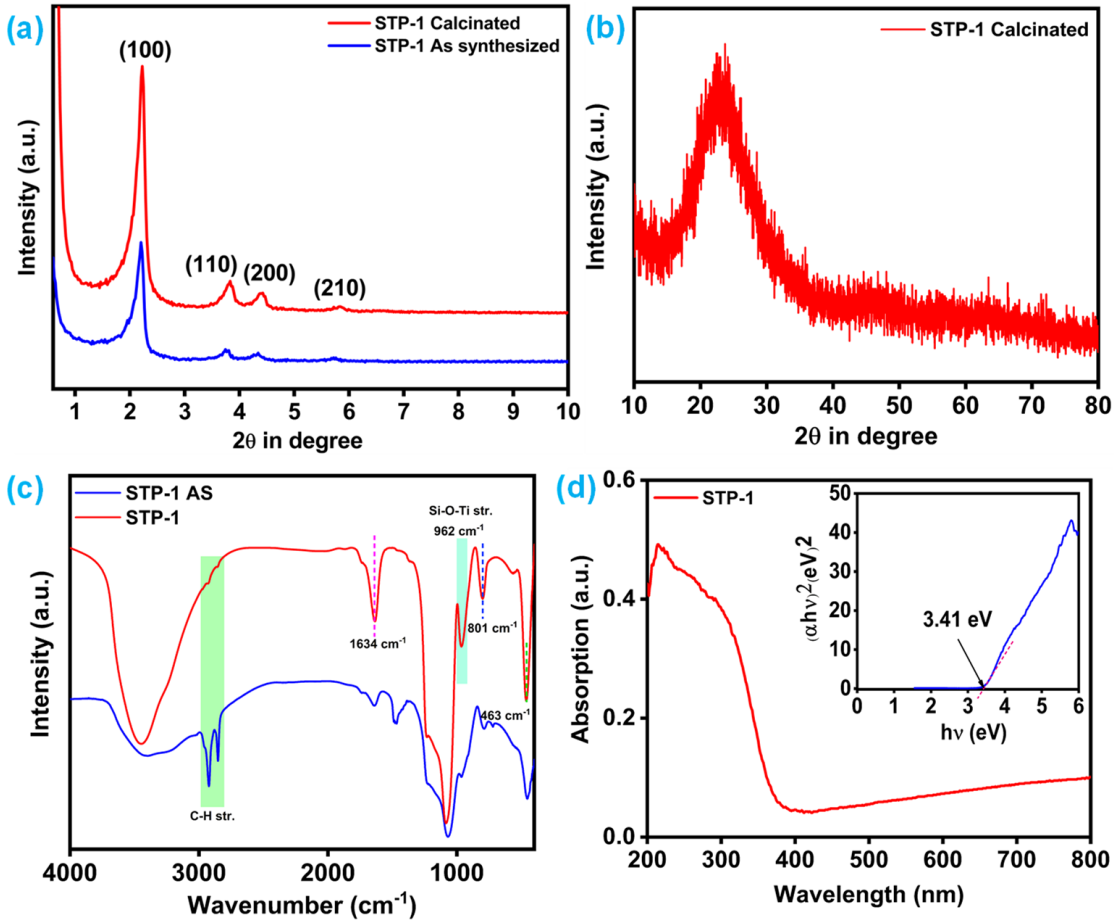

Figure 1. (**a**) Small-angle powder XRD pattern of the as-synthesized and calcinated STP-1; (**b**) wide-angle powder XRD pattern of the calcinated STP-1 material; (**c**) FT-IR spectra of the as-synthesized (blue) and calcinated (red) STP-1; (**d**) UV-Vis DRS data of STP-1 (Tauc plot as the inset).

FT-IR spectra of KBr palletized as the synthesis and calcined STP-1 samples are shown in Figure 1c. A strong band at 962 cm^{-1} was associated to tetrahedral Ti unit (Si-O-Ti stretching), which was incorporated into the silica framework [39]. The as-synthesized STP-1 material showed two peaks at 2923 and 2843 cm^{-1} due to the C-H bond stretching, as this sample contained a CTAB template. However, these peaks disappeared in the calcined STP-1 material. A characteristic broad peak appearing at 3300–3750 cm^{-1} confirmed the –OH group of silanol overlapped with absorbed water molecules. A band at 1634 cm^{-1} was also observed due to Ti-O-Si lattice overtones. For symmetric stretching and bending of Si-O bonds, two bands appeared at 801 and 463 cm^{-1}, respectively [40].

Raman spectroscopy is an important tool for the identification of coordination environment of titanium atoms in the mesoporous silica framework. The Raman spectrum shown in Figure S3 supports the structural feature associated with the STP-1 material. The presence of the peaks at 504.5 and 1083 cm^{-1} could be assigned due to the asymmetric stretching of the Si-O-Si unit [41]. The peak at 627 cm^{-1} signified Ti-O-Ti [42], and the peaks at 485, 515, and 1125 cm^{-1} signified the presence of the Si-O-Ti moiety [43].

UV-visible diffused reflectance spectra (DRS) is extensively used to characterized the coordination environment of titanium into the silica framework. The UV-Vis DR spectra of STP-1 (Figure 1d) showed a broad absorption in the range of 210–220 nm, which could be attributed to a strong absorption peak for the ligand-to-metal charge transfer (LMCT) from O^{2-} to Ti^{4+} [44]. From the Tauc plot, we also calculated the band gap of STP-1 that came at 3.41 eV, which also suggested that TiO_2 was not formed [45].

The analysis of the permanent porosity inside the architecture of STP-1 was carried out through N_2 sorption analysis at 77 K. The Brunauer-Emmett-Teller (BET) isotherm represented in Figure 2a belonged to the classical type IV isotherm [46] according to IUPAC classification. The sharp N_2 uptake at a lower-pressure region and no hysteresis indication of the capillary condensation clearly supported the formation of silica mesophase [47]. The pore size distribution analysis (Figure 2b) carried out using the nonlocal density functional theory (NLDFT) conferred the presence of mesopores with a pore size of 4.4 nm. The BET surface area of the material was found to be 878 m^2/g. The pore volume of the material was 0.75 cc/g.

The morphological analysis of the calcinated STP-1 sample was performed by high-resolution transmission electron microscopy (TEM) and scanning electron microscopy (SEM) analysis. The TEM images obtained in lower resolution indicated the formation of spherical nanoparticle assembly with a particle size of 0.8 µm (Figure 2d(i)). By increasing the resolution, the images (Figure 2d(ii–iv)) clearly indicated hollowness in particles. This result suggested the high specific area of the materials. The high-resolution TEM images clearly revealed the crystal fringe pattern (Figure 2d(v,vi)) with a fringe width of 3.96 nm, which was also supported by the small-angle PXRD pattern. To obtain further insights of the morphological feature, we carried out the scanning electron microscopic analysis. The SEM images also clearly confirmed the presence of a hollow globular morphology with the particle sizes of 0.5–0.8 µm (Figure 2c(i–iv)) [48]. The elemental mapping images obtained from the TEM analysis confirmed uniform distributions of Ti, Si, O, and P all over the material (Figure S4). The titanium amount in STP-1 was calculated as Ti/Si = 0.006 from energy-dispersive X-ray spectroscopic analysis (EDX). The characterization results (small angle PXRD and FT-IR) of the phosphate modified mesoporous silica without titanium (SP-1) is provided in supporting information file (Figures S1 and S2).

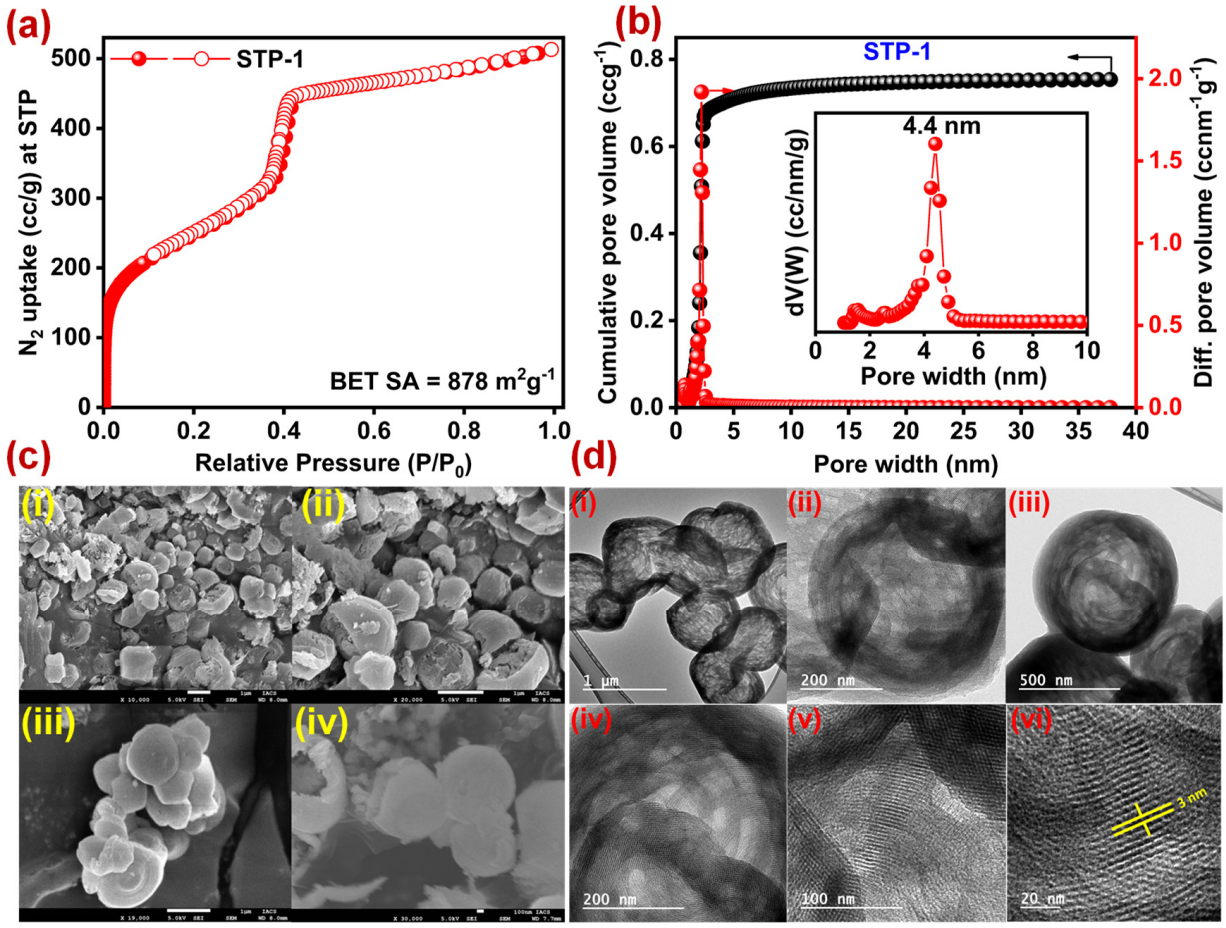

Figure 2. (**a**) N_2 sorption isotherm of STP-1 at 77 K; (**b**) pore size distribution of STP-1 by using the NLDFT method; (**c**) SEM images (**i**–**iv**) of STP-1; (**d**) TEM images (**i**–**vi**) of STP-1.

4. Discussion

4.1. Catalysis

After the successful incorporation of Ti on the phosphate-modified mesoporous silica framework, it was employed as a catalyst for the classical oxidation of styrene (Scheme 1). A harsh reaction condition was used for the oxidation of styrene to form benzaldehyde, but the major challenge was to attain high selectivity. Here, we have performed all the reactions under mild reaction conditions using dilute aqueous H_2O_2 as an oxidant. All the parameters, which governed the reaction such as the temperature, the reaction time, and the molar ratio of H_2O_2 were thoroughly studied. To assess the catalytic role of STP-1, a blank test was performed (Table 1, entry 1), which gave only a 3.2% conversion with moderate selectivity after a 5 h reaction time. When pure silica MCM-41 was used as a catalyst, it did not give any noticeable conversion of styrene in this oxidation reaction. Therefore, in this study, we systematically optimized all the parameters step by step. Initially, in the presence of a 10% catalyst loading, we achieved a 16.15% conversion after 5 h reaction (Table 1, entry 9). This investigation also suggested that the selectivity is obvious for benzaldehyde and subtle for styrene oxide. It is important to note that the selectivity also increased over the time (Table 1, entries 2–6). The other byproducts such as phenylacetaldehyde, formaldehyde, and benzoic acid also formed during the reaction, and these were quantified from the GC analysis (Figures S7–S11). As a moderate conversion was achieved by increasing the reaction time at 70 °C (Table 1, entries 2–6), the reaction was further performed in 80 °C under the same catalyst loading. A time-dependent analysis clearly demonstrated that there was no significant conversion beyond 4 h (Table 1, entry 10). Again, when the reaction was conducted at an 80 °C temperature,

a huge byproduct formation was observed by increasing the reaction time. Both the blank test and the reaction at an 80 °C temperature indicated the role of the phase of the catalyst on the benzaldehyde selectivity and suggested that 70 °C is the optimum temperature for this liquid phase oxidation reaction. To achieve the higher selectivity of benzaldehyde, we increased the molar ratio of H_2O_2 under the same reaction conditions. Entries 11–13 showed that a considerable conversion of styrene with a 93.8% selectivity of benzaldehyde could be achieved when the reaction was conducted at 70 °C for 10 h. We also checked the catalytic activity of STP-1 in the presence of oxygen instead of H_2O_2, which did not give satisfactory results (Table 1, entry 14). The high benzaldehyde selectivity over STP-1 catalyst also suggested a synergistic effect of phosphorous and titanium into the mesoporous silica framework. We also conducted the styrene oxidation reaction over only phosphate-modified mesoporous silica material SP-1, which gave a 6.61% conversion with a 71.6% benzaldehyde selectivity (Table 1, entry 15). This result clearly indicated that there was some impact of phosphorous in this catalytic reaction. Hulea et al. showed that various Ti-containing molecular sieves, i.e., TS-1, Ti-beta, and Ti-MCM-41, gave different product selectivities [45]. Phenyl acetic acid was selectively formed when styrene oxidation performed over TS-1, whereas benzaldehyde formed as a major product over Ti-beta and Ti-MCM-41 catalysts. This observation suggested that the selectivity of the product in styrene oxidation reaction is highly dependent on the topology of the frameworks. We also compared this finding to the results of other catalysts, and these are shown in Table 2. Various types of mesoporous titanium silicate-based catalysts were used in this liquid phase styrene oxidation reaction, including Ti-doped and Ti/Fe-doped catalysts, which gave moderate yields together with low benzaldehyde selectivity. TS-1 showed a selectivity of 26.5% for benzaldehyde, which was considerably low when compared to that of the Ti-MCM-41 counterpart. Ti-SBA-15-based materials were also employed for this reaction; a significant conversion was observed, but the selectivity was not quite high. Both the yield and the selectivity were also insufficient over MOF-based materials. Thus, our catalytic results on STP-1 suggested that the phosphate modification on Ti-MCM-41 is very important for obtaining high selectivity for benzaldehyde in this liquid phase styrene oxidation reaction. From this observation, we can infer that the synergistic assembly of both titanium and phosphate plays a more crucial role than the individual one in the overall catalysis.

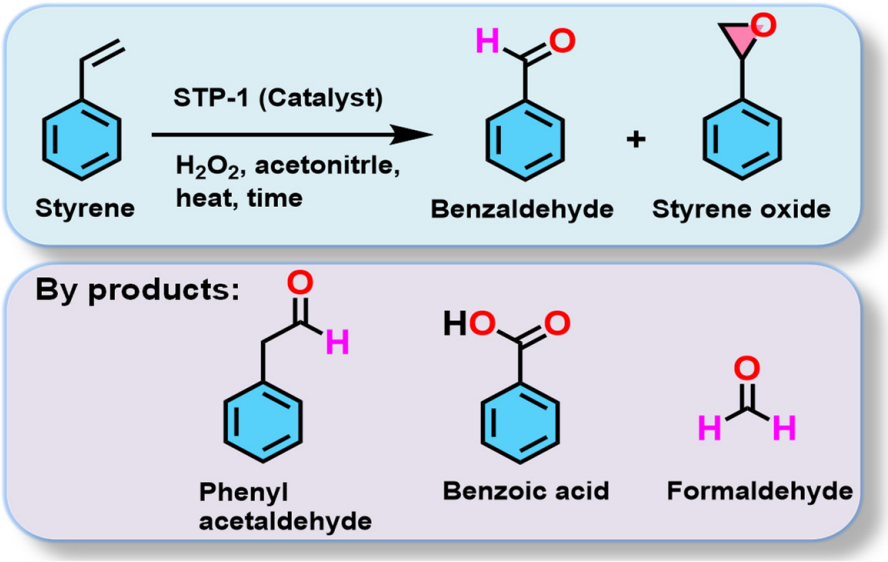

Scheme 1. Oxidation of styrene over STP-1.

Table 1. Optimization table for the liquid phase oxidation of styrene over STP-1.

Entry	Catalyst	Catalyst Amount (wt%)	Temperature (°C)	Time (h)	Conversion (%)	SO Selectivity (%)	BA Selectivity (%)
1	Blank	-	70	5	3.2	9.6	67.3
2	STP-1	10	70	1	4.4	8.7	70.1
3	STP-1	10	70	2	9.1	7.8	63.7
4	STP-1	10	70	3	11.9	9.6	86.2
5	STP-1	10	70	4	13.5	6.5	89.3
6	STP-1	10	70	5	16.5	5.2	84.5
7	STP-1	10	80	1	7.6	7.9	60.0
8	STP-1	10	80	2	8.4	7.5	50.5
9	STP-1	10	80	3	16.1	10.5	73.0
10	STP-1	10	80	4	20.7	7.5	53.1
11 [a]	STP-1	10	80	10	25.2	6.3	47.2
12 [a]	STP-1	10	70	5	29.1	3.9	48.6
13 [a]	**STP-1**	**10**	**70**	**10**	**32.8**	**4.6**	**93.8**
14 [b]	STP-1	10	70	10	0.6	n.d	20.2
15 [c]	SP-1	10	70	10	6.6	22.5	71.6

Reaction conditions: styrene (5 mmol), H_2O_2 (5 mmol), catalyst (10 wt%), and solvent acetonitile (5 mL). [a]: Styrene (5 mmol), H_2O_2 (10 mmol), catalyst (10 wt%), solvent acetonitile (5 mL). [b]: An oxygen atmosphere was used instead of H_2O_2. (n.d. refers to not detected). [c]: phosphate modified mesoporous silica without titanium (SP-1) was used as a catalyst.

Table 2. Comparison study with the previously reported state-of-the-art catalysts.

Entry	Catalyst	Reaction Condition	Styrene Conversion (%)	Benzaldehyde Selectivity (%)	Ref.
1	Ti-MCM-41 (H_2O_2)	70 °C, 5 h	26.1	52.3	[45]
2	Ti-Fe-MCM-41 (H_2O_2)	70 °C, 12 h	50	90.1	[49]
3	TS-1 (H_2O_2)	70 °C, 5 h	21.1	26.5	[45]
4	$H_3PW_{12}O_{40}$/SBA-15 (H_2O_2)	70 °C, 24 h	22.6	100	[50]
5	CoVSB-5 (H_2O_2)	70 °C, 6 h	57	75	[51]
6	Ti-Fe-SBA-15 (H_2O_2)	70 °C, 12 h	37.1	86.3	[49]
7	Ti-beta (H_2O_2)	70 °C, 5 h	20.1	57.2	[45]
8	SiO_2 (H_2O_2)	50 °C, 6 h	-	-	[48]
9	1.97% CeO_2-SiO_2	50 °C, 6 h	42.9	42.90	[48]
10	0.98% CeO_2-SiO_2	50 °C, 12 h	81.40	27.30	[48]
11	Ni/SiO_2 (H_2O_2)	75 °C, 12 h	31.2	90.20	[52]
12	FePcS/NH_2-MCM-48	RT, 6 h	21.9	23.90	[53]
13	FePcS/NH_2-MCM-48	RT, 24 h	65.5	21.4	[53]
14	MIL@NTU-1 (TBHP)	80 °C, 12 h	31.4	12	[54]
15	**STP-1 (H_2O_2)**	**70 °C, 10 h**	**32.7**	**93.8**	**This work**

4.2. Plausible Reaction Mechanism

In the styrene oxidation reaction over STP-1 catalyst by using H_2O_2, the free radical mechanism involves the interaction of H_2O_2 with the tetrahedrally coordinated Ti (A), which is nicely dispersed into the silica framework. After that tetradedrally coordinated Ti into the silica framework (A), species interact with H_2O_2 to form highly reactive hydroperoxyl species (B). This hydroperoxyl species (B) species reduces one electron to form Ti peroxo species (C) [Ti(IV)-O˙ radical] and removes a water molecule. This Ti-peroxo species (C) interacts with the π-bond of styrene and produce styrene oxide. The C=C bond cleavage of styrene occurs to produce benzaldehyde via the radical transformation reaction due to the presence of polar water molecules. Lubis et al. nicely presented that this overall reaction pathways occurs through free radical mechanism [55]. In addition, the isomerization of styrene oxide produces phenyl acetaldehyde [56]. The overall proposed selective oxidation reaction pathway in the presence of H_2O_2 is shown in Figure 3.

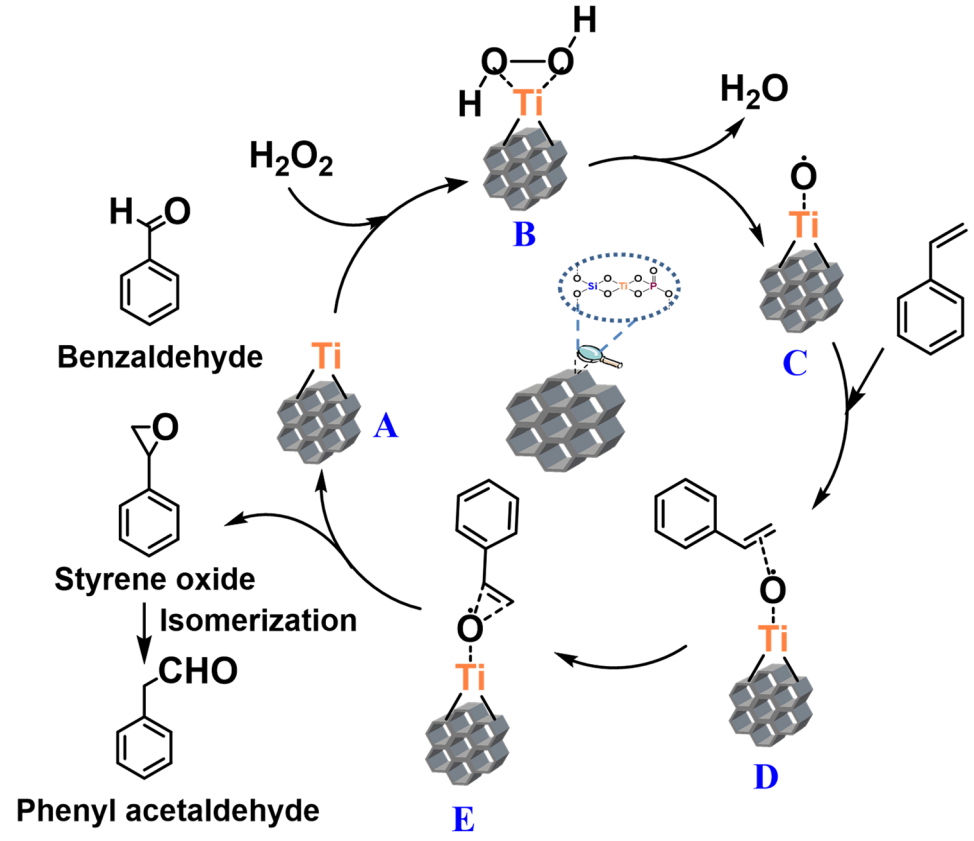

Figure 3. Plausible mechanistic pathway of styrene oxidation over STP-1.

4.3. Recyclability Test

A recyclability experiment was also carried out in order to check the heterogeneity of the catalyst. To carry out the catalytic recyclability experiment, we chose the optimized reaction condition for selective styrene oxidation over STP-1 catalyst. After each of the reaction cycles, the catalyst was separated from the reaction mixture by a simple centrifugation process; after that, the catalyst was dried at a 150 °C hot air oven for 2 h and used for next catalytic cycle. It was observed that there was no significant change in selectivity up to five cycles (Figure 4). After the completion of five cycles, small-angle powder XRD, FT-IR, and SEM analyses were carried out, and these did not show any noticeable changes (Figures S5 and S6). All the collective experimental results confirmed the robustness of this mesoporous phosphate-modified titanium silicate (STP-1) catalyst and used as a potential candidate for the selective conversion of styrene oxide.

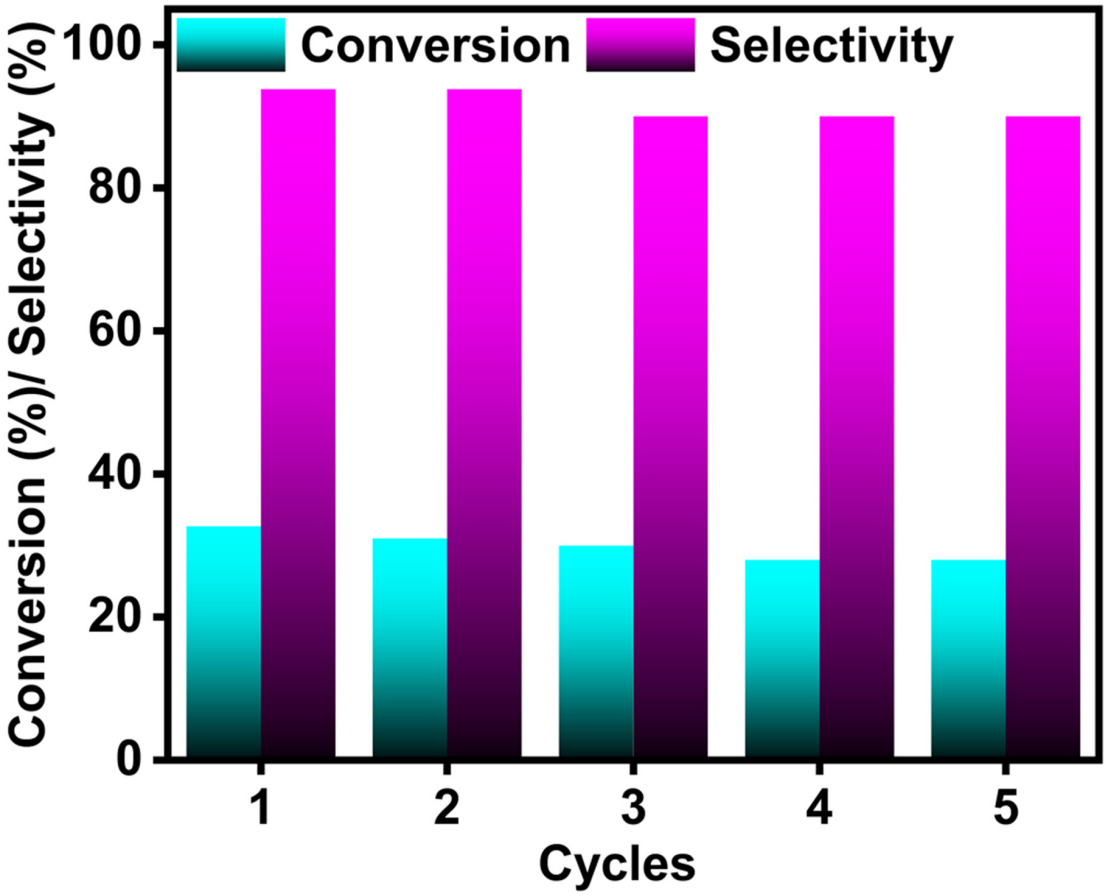

Figure 4. Recycling ability of STP-1 catalyst in the liquid phase oxidation of styrene to benzaldehyde.

5. Conclusions

In conclusion, we have synthesized a Ti-incorporated mesoporous silica molecular sieve through a novel phosphate modification strategy. The mesoporous phosphate-modified titanium silicate material STP-1 showed a 2D-hexagonal mesoporous nanostructure with a pore diameter of 4.4 nm and a very high specific surface area of 838 m^2g^{-1}. STP-1 was successfully utilized in the selective styrene oxidation using dilute aqueous H_2O_2 as a peroxide source. The incorporated Ti inside the silica matrix was involved in this C-C bond cleavage under mild liquid phase conditions. Optimization studies suggested good conversion of styrene with a 93.8% selectivity for benzaldehyde. We have also shown that phosphate-modified mesoporous silica gave only a 6.6% styrene conversion and a 71.6% benzaldehyde selectivity. These results suggest that incorporating phosphate and titanium into the silica framework synergistically plays an important role in forming highly selective benzaldehyde products. These results also suggest that phosphate-modified mesoporous titanium silicate can be a promising catalyst for the selective oxidation of organics for the sustainable and cost-effective synthesis of valuable fine chemicals.

Supplementary Materials: The following supporting information can be downloaded at: https://www.mdpi.com/article/10.3390/chemistry5010042/s1, Figure S1: Small-angle powder XRD data of SP-1; Figure S2: FT-IR spectra of SP-1; Figure S3: Raman spectra of STP-1 sample; Figure S4: Elemental mapping of STP-1; Figure S5: FT-IR spectra of STP-1 catalyst after 5 catalytic cycles; Figure S6: SEM image after 5 catalytic cycles; Figure S7: GC-FID data of the styrene oxidation reaction mixture after 1 h by STP-1 catalyst; Figure S8: GC-FID data of the styrene oxidation reaction mixture after 2 h by STP-1 catalyst; Figure S9: GC-FID data of the styrene oxidation reaction mixture after 5 h by STP-1 catalyst; Figure S10: GC-FID data of the styrene oxidation reaction mixture after 10 h by STP-1 catalyst with O_2 used as an oxidant; Figure S11: GC-FID data of the styrene oxidation reaction mixture after 10 h by SP-1 catalyst by H_2O_2.

Author Contributions: Experiments, investigation and formal analysis were performed by R.C., A.C. and S.B. R.B. was involved in formal analysis. A.B. provided the resources, investigation, write-up, and overall supervision of this project. All authors have read and agreed to the published version of the manuscript.

Funding: This work is partly funded by DST-SERB through a core research grant (project No. CRG/2022/002812).

Institutional Review Board Statement: Not applicable.

Informed Consent Statement: Not applicable.

Data Availability Statement: Not applicable.

Acknowledgments: R.C. and A.C. would like to thank CSIR, New Delhi for their respective senior research fellowships. S.B. would like to thank IGSTC, New Delhi for a senior research fellowship.

Conflicts of Interest: The authors declare no conflict of interest.

References

1. Trost, B.M. *Comprehensive Organic Synthesis*; Pergamon: New York, NY, USA, 1991.
2. Corma, A.; Serra, J.M.; Serna, P.; Valero, S.; Argente, E.; Botti, V. Optimisation of olefin epoxidation catalysts with the application of high-throughput and genetic algorithms assisted by artificial neural networks (softcomputing techniques). *J. Catal.* **2005**, *229*, 513–524. [CrossRef]
3. Parker, R.E.; Isaacs, N.S. Mechanisms of Epoxide Reactions. *Chem. Rev.* **1959**, *59*, 737–799. [CrossRef]
4. Corma, A.; Navarro, M.T.; Pariente, J.P. Synthesis of an Ultralarge Pore Titanium Silicate Isomorphous to MCM-41 and Its Application as a Catalyst for Selective Oxidation of Hydrocarbons. *J. Chem. Soc. Chem. Commun.* **1994**, *2*, 147–148. [CrossRef]
5. Bhaumik, A.; Kumar, R. Titanium silicate molecular sieve (TS-1)/H2O2 induced triphase catalysis in the oxidation of hydrophobic organic compounds with significant enhancement of activity and para selectivity. *J. Chem. Soc. Chem. Commun.* **1995**, *3*, 249–250. [CrossRef]
6. Kholdeeva, O.; Maksimchuk, N. Metal-Organic Frameworks in Oxidation Catalysis with Hydrogen Peroxide. *Catalysts* **2021**, *11*, 283. [CrossRef]
7. Bailey, P.S.; Hwang, H.H.; Chiang, C.Y. Mechanisms of Epoxidation during Ozonation of Carbon-Carbon Double Bonds. *J. Org. Chem.* **1985**, *50*, 231–234. [CrossRef]
8. Yu, W.; Zhao, Z. Catalyst-Free Selective Oxidation of Diverse Olefins to Carbonyls in High Yield Enabled by Light under Mild Conditions. *Org. Lett.* **2019**, *21*, 7726–7730. [CrossRef] [PubMed]
9. Murphy, A.; Dubois, G.; Stack, T.D.P. Efficient Epoxidation of Electron-Deficient Olefins with a Cationic Manganese Complex. *J. Am. Chem. Soc.* **2003**, *125*, 5250–5251. [CrossRef] [PubMed]
10. Corma, A.; Garcia, H. Supported gold nanoparticles as catalysts for organic reactions. *Chem. Soc. Rev.* **2008**, *37*, 2096–2126. [CrossRef]
11. Bhaumik, A.; Mukherjee, P.; Kumar, R. Triphase catalysis over titanium-silicate molecular sieves under solvent-free conditions—I. Direct hydroxylation of benzene. *J. Catal.* **1998**, *178*, 101–107. [CrossRef]
12. Drozd, V.A.; Ottenbacher, R.V.; Bryliakov, K.P. Asymmetric Epoxidation of Olefins with Sodium Percarbonate Catalyzed by Bis-Amino-Bis-Pyridine Manganese Complexes. *Molecules* **2022**, *27*, 2538. [CrossRef]
13. Sun, C.; Liu, H. Highly Selective Oxidation of styrene to styrene Oxide over a Tetraphenylporphyrin-Bridged Silsesquioxane-Based Hybrid Porous Polymer. *ACS Appl. Mater. Interfaces* **2022**, *4*, 5471–5481. [CrossRef]
14. Liu, R.; Qu, J. Review on heterogeneous oxidation and adsorption for arsenic removal from drinking water. *J. Environ. Sci.* **2021**, *110*, 178–188. [CrossRef]
15. Jørgensen, K.A. Transition-Metal-Catalyzed Epoxidations. *Chem. Rev.* **1989**, *89*, 431–458. [CrossRef]
16. Sheldon, R.A.; Van Doorn, J.A. Metal-Catalyzed Epoxidation of Olefins with Organic Hydroperoxides. I. A Comparison of Various Metal Catalysts. *J. Catal.* **1973**, *31*, 427–437. [CrossRef]
17. Xu, D.; Sun, Q.; Lin, J.; Sun, W. Ligand Regulation for Manganese-Catalyzed Enantioselective Epoxidation of Olefins without Acid. *Chem. Commun.* **2020**, *56*, 13101–13104. [CrossRef] [PubMed]
18. Lyons, J.E. Oxidation of Olefins in the Presence of Transition Metal Complexes. *Adv. Chem. Ser.* **1974**, *132*, 64–89.
19. Oloo, W.N.; Banerjee, R.; Lipscomb, J.D.; Que, L. Equilibrating (L)Fe^{III}–OOAc and (L)Fe^{V}(O) Species in Hydrocarbon Oxidations by Bio-Inspired Nonheme Iron Catalysts Using H_2O_2 and AcOH. *J. Am. Chem. Soc.* **2017**, *139*, 17313–17326. [CrossRef]
20. Dumesic, J.A.; Huber, G.W. Catalysis Science & Technology Ethylene Oligomerization into Linear Olefins. *Catal. Sci. Technol.* **2022**, *12*, 3639–3649.
21. Xiong, C.; Liang, Y.; Zhou, X.; Xue, C.; Ji, H. Facile Synthesis of a Mo-Based TiO_2 Catalyst via a Redox Strategy for High Value-Added Conversion of Olefin. *Fuel* **2023**, *332*, 126172. [CrossRef]
22. Jibowu, T. A Review on Nanoporous Metals. *Front. Nanosci. Nanotechnol.* **2016**, *2*, 165–168. [CrossRef]

23. Chen, D.M.; Zhang, X.J. Enhancing the Stability of Metal-Organic Framework via Ligand Modification: Scalable Synthesis and High Selectivity of CO_2 Sorption Property. *CrystEngComm* **2022**, *25*, 467–472. [CrossRef]
24. Song, B.Y.; Zhang, X.F.; Huang, J.; Cheng, X.L.; Deng, Z.P.; Xu, Y.M.; Huo, L.H.; Gao, S. Porous Cr_2O_3 Architecture Assembled by Nano-Sized Cylinders/Ellipsoids for Enhanced Sensing to Trace H_2S Gas. *ACS Appl. Mater. Interfaces* **2022**, *14*, 22302–22312. [CrossRef] [PubMed]
25. Sodha, V.; Shahabuddin, S.; Gaur, R.; Ahmad, I.; Bandyopadhyay, R.; Sridewi, N. Comprehensive Review on Zeolite-Based Nanocomposites for Treatment of Effluents from Wastewater. *Nanomaterials* **2022**, *12*, 3199. [CrossRef] [PubMed]
26. Zhu, N.X.; Wei, Z.W.; Chen, C.X.; Xiong, X.H.; Xiong, Y.Y.; Zeng, Z.; Wang, W.; Jiang, J.J.; Fan, Y.N.; Su, C.Y. High Water Adsorption MOFs with Optimized Pore-Nanospaces for Autonomous Indoor Humidity Control and Pollutants Removal. *Angew. Chem. Int. Ed.* **2022**, *61*, e202112097.
27. Kresge, C.T.; Leonowicz, M.E.; Roth, W.J.; Vartuli, J.C.; Beckt, J.S. Ordered Mesoporous Molecular Sieves Synthesized by a Liquid-Crystal Template Mechanism. *Nature* **1992**, *359*, 710–712. [CrossRef]
28. Zhao, D.; Feng, J.; Huo, Q.; Melosh, N.; Fredrickson, G.H.; Chmelka, B.F.; Stucky, G.D. Triblock Copolymer Syntheses of Mesoporous Silica with Periodic 50 to 300 Angstrom Pores. *Science* **1998**, *279*, 548–552. [CrossRef] [PubMed]
29. Mesa, M.; Sierra, L.; Patarin, J.; Guth, J. Morphology and Porosity Characteristics Control of SBA-16 Mesoporous Silica. Effect of the Triblock Surfactant Pluronic F127 Degradation during the Synthesis. *Solid State Sci.* **2005**, *7*, 990–997. [CrossRef]
30. Kim, J.M.; Kim, S.K.; Ryoo, R. Synthesis of MCM-48 Single Crystals. *Chem. Commun.* **1998**, *1*, 259–260. [CrossRef]
31. Bonino, F.; Damin, A.; Ricchiardi, G.; Ricci, M.; Spano, G.; D'Aloisio, R.; Zecchina, A.; Lamberti, C.; Prestipino, C.; Bordiga, S. Ti-peroxo species in the TS-1/H_2O_2/H_2O system. *J. Phys. Chem. B* **2004**, *108*, 3573–3583. [CrossRef]
32. Gordon, C.P.; Engler, H.; Tragl, A.S.; Plodinec, M.; Lunkenbein, T.; Berkessel, A.; Teles, J.H.; Parvulescu, A.N.; Coperet, C. Efficient epoxidation over dinuclear sites in titanium silicalite-1. *Nature* **2020**, *586*, 708–710. [CrossRef]
33. Zhang, M.; Ren, S.Y.; Guo, Q.X.; Shen, B.J. Synthesis of hierarchically porous zeolite TS-1 with small crystal size and its performance of 1-hexene epoxidation reaction. *Microporous Mesoporous Mater.* **2021**, *326*, 111395. [CrossRef]
34. Bhaumik, A.; Inagaki, S. Mesoporous titanium phosphate molecular sieves with ion-exchange capacity. *J. Am. Chem. Soc.* **2001**, *123*, 691–696. [CrossRef]
35. Alvaro, M.; Corma, A.; Das, D.; Fornes, V.; Garcia, H. "Nafion"—functionalized mesoporous MCM-41 silica shows high activity and selectivity for carboxylic acid esterification and Friedel-Crafts acylation reactions. *J. Catal.* **2005**, *231*, 48–55. [CrossRef]
36. Beck, J.S.; Vartuli, J.C.; Roth, W.J.; Leonowicz, M.E.; Kresge, C.T.; Schmitt, K.D.; Chu, C.T.W.; Olson, D.H.; Sheppard, E.W.; McCullen, S.B.; et al. A New Family of Mesoporous Molecular Sieves Prepared with Liquid Crystal Templates. *J. Am. Chem. Soc.* **1992**, *114*, 10834–10843. [CrossRef]
37. Bhaumik, A.; Tatsumi, T. Organically Modified Titanium-Rich Ti-MCM-41, Efficient Catalysts for Epoxidation Reactions. *J. Catal.* **2000**, *189*, 31–39. [CrossRef]
38. Peng, R.; Zhao, D.; Dimitrijevic, N.M.; Rajh, T.; Koodali, R.T. Room Temperature Synthesis of Ti-MCM-48 and Ti-MCM-41 Mesoporous Materials and Their Performance on Photocatalytic Splitting of Water. *J. Phys. Chem. C* **2012**, *116*, 1605–1613. [CrossRef]
39. Rhee, C.H.; Lee, J.S. Preparation and Characterization of Titanium-Substituted MCM-41. *Catal. Today* **1997**, *38*, 213–219. [CrossRef]
40. Schacht, P.; Noreña-Franco, L.; Ancheyta, J.; Ramírez, S.; Hernández-Pérez, I.; García, L.A. Characterization of Hydrothermally Treated MCM-41 and Ti-MCM-41 Molecular Sieves. *Catal. Today* **2004**, *98*, 115–121. [CrossRef]
41. Yu, J.; Feng, Z.; Xu, L.; Li, M.; Xin, Q.; Liu, Z. Ti-MCM-41 Synthesized from Colloidal Silica and Titanium Trichloride: Synthesis, Characterization, and Catalysis. *Chem. Mater.* **2001**, *13*, 994–998. [CrossRef]
42. Petersen, H.; Stegmann, N.; Fischer, M.; Zibrowius, B.; Radev, I.; Philippi, W.; Schmidt, W.; Weidenthaler, C. Crystal Structures of Two Titanium Phosphate-Based Proton Conductors: Ab Initio Structure Solution and Materials Properties. *Inorg. Chem.* **2022**, *61*, 2379–2390. [CrossRef]
43. Li, C.; Xiong, G.; Xin, Q.; Liu, J.; Ying, P.; Feng, Z.; Li, J.; Yang, W.; Wang, Y.; Wang, G.; et al. UV Resonance Raman Spectroscopic Identification of Titanium Atoms in the Framework of TS-1 Zeolite. *Angew. Chem. Int. Ed.* **1999**, *38*, 2220–2222. [CrossRef]
44. Boccuti, M.R.; Raol, K.M.; Zecchina, A.; Leofanti, G.; Petrini, G. Spectroscopic Characterization of Silicalite And Titanium-Silicalite. *Struct. React. Surf.* **1989**, *48*, 133–144.
45. Hulea, V.; Dumitriu, E. Styrene Oxidation with H_2O_2 over Ti-Containing Molecular Sieves with MFI, BEA and MCM-41 Topologies. *Appl. Catal. A Gen.* **2004**, *277*, 99–106. [CrossRef]
46. Das, S.; Chatterjee, S.; Mondal, S.; Modak, A.; Chandra, B.K.; Das, S.; Nessim, G.D.; Majee, A.; Bhaumik, A. Thiadiazole Containing N- and S-Rich Highly Ordered Periodic Mesoporous Organosilica for Efficient Removal of Hg(II) from Polluted Water. *Chem. Commun.* **2020**, *56*, 3963–3966. [CrossRef] [PubMed]
47. Ghosh, A.; Chowdhury, B.; Bhaumik, A. Synthesis of Hollow Mesoporous Silica Nanospheroids with O/W Emulsion and Al(III) Incorporation and Its Catalytic. *Catalysts* **2023**, *13*, 354. [CrossRef]
48. Sarkar, B.; Singha, R.K.; Tiwari, R.; Ghosh, S. Preparation of CeO_2 Nanoparticles Supported on 1-D Silica Nanostructures for Room Temperature Selective Oxidation of Styrene. *RSC Adv.* **2014**, *4*, 5453–5456. [CrossRef]
49. Wu, Y.; Zhang, Y.; Cheng, J.; Li, Z.; Wang, H.; Sun, Q.; Han, B. Microporous and Mesoporous Materials Synthesis, Characterization and Catalytic Activity of Binary Metallic Titanium and Iron Containing Mesoporous Silica. *Microporous Mesoporous Mater.* **2012**, *162*, 51–59. [CrossRef]

50. Sun, W.; Hu, J. Oxidation of Styrene to Benzaldehyde with Hydrogen Peroxide in the Presence of Catalysts Obtained by the Immobilization of H 3 PW 12 O 40 on SBA-15 Mesoporous Material. *React. Kinet. Mech. Catal.* **2016**, *119*, 305–318. [CrossRef]
51. Gao, D.; Gao, Q. Selective Oxidation of Styrene to Benzaldehyde over VSB-5 and Isomorphously Substituted Cobalt VSB-5. *Catal. Commun.* **2007**, *8*, 681–685. [CrossRef]
52. Liu, J.; Chen, T.; Jian, P.; Wang, L. Journal of Colloid and Interface Science Hierarchical Hollow Nickel Silicate Microflowers for Selective Oxidation of Styrene. *J. Colloid Interface Sci.* **2019**, *553*, 606–612. [CrossRef] [PubMed]
53. Pirouzmand, M.; Amini, M.M.; Safari, N. Immobilization of Iron Tetrasulfophthalocyanine on Functionalized MCM-48 and MCM-41 Mesoporous Silicas: Catalysts for Oxidation of Styrene. *J. Colloid Interface Sci.* **2008**, *319*, 199–205. [CrossRef] [PubMed]
54. Cai, M.; Li, Y.; Liu, Q.; Xue, Z.; Wang, H.; Fan, Y.; Zhu, K. One-Step Construction of Hydrophobic MOFs @ COFs Core—Shell Composites for Heterogeneous Selective Catalysis. *Adv. Sci.* **2019**, *1802365*, 1802365. [CrossRef] [PubMed]
55. Lubis, S.; Yuliati, L.; Lee, S.L.; Sumpono, I.; Nur, H. Improvement of Catalytic Activity in Styrene Oxidation of Carbon-Coated Titania by Formation of Porous Carbon Layer. *Chem. Eng. J.* **2012**, *209*, 486–493. [CrossRef]
56. Lignier, P.; Mangematin, S.; Morfin, F.; Rousset, J.L.; Caps, V. Solvent and Oxidant Effects on the Au/TiO_2—Catalyzed Aerobic Epoxidation of Stilbene. *Catal. Today* **2008**, *138*, 50–54. [CrossRef]